Estimation of Normal Pressure at Tool-chip Interface Based on Finite Element Method (FEM)

Maan Aabid Tawfiq*

Received on: 17/5/2005
Accepted on: 7/9/2005

Abstract

The main objective of this study is to investigate the effect of rake angle on normal pressure distribution at tool-chip interface region, in order to gain better understanding of the rake angle effects in orthogonal cutting with continuous chip formation. The effect of normal pressure at tool-chip interface for (AISI 1045 St) has been studied for cutting tools having various rake angles, which are modeled and simulated. Special FEM codes are applied, the first code is:(MSC FEA/PATRAN/2004), used for preprocessing & postprocessing, while the second one is (MSC FEA/DYTRAN /2004), used for the analysis stage. Finite Element model sets for steady state orthogonal cutting are presented. The model simulates chip formation process in detail.

The modeling and simulation process is based on certain criteria called "Johnson-Cook" constitutive model for predicting dynamic material behavior, so the flow stress of the chip is taken as a function of strain hardening, strain rate and temperature. It is concluded from the simulated results, that the normal pressure is minimum when the rake angle is (5^{o}), while the normal pressure is maximum when the rake angle is (-15^{o}). Pressure distribution and behavior at this region are studied in detail. The results are compared with many relevant papers published in the literature and showed a good agreement with the modeled results.

Keywords: FEM, Tool-Chip interface, Normal Pressure, Machining.

حساب الضغط العمودي في منطقة تماس وجه العدة مع النحاته باستخدام طريقة العناصر المحدده

الخلاصة

يهدف هذا البحث الى دراسة تأثير زاوية الجرف لعدة القطع على توزيع الضغط العمودي في منطقة تماس وجه عدة القطع مع النحاته (الرايش)، وذلك بهدف دراسة أشمل لتأثيرات هذه الزاوية في حالة القطع المتعامد عند ظروف ظهور النحاته المستمرة. تم في هذا البحث أخذ قيم مختلفة من زوايا جرف عدة القطع وذلك بنمذجة ومحاكاة عملية القطع لصلب نوع (AISI 1045St.)باستخدام برنامجين حاسوبيين خاصين يستخدمان طريقة العناصر المحددة (FEM). اما البرنامج الاول فهو (MSC FEA/PATRAN/2004) فقد تم استخدامه لعمليتي المعالجة البدائية والمتقدمة، في حين تم استخدام البرنامج الثاني ويدعى(MSC FEA/DYTRAN /2004) وذلك لاجراء عمليات التحليل الرياضي. تم عرض مجموعة من الموديلات بطريقة العناصر المحددة لهذا الغرض وذلك عند ظروف مستقرة للقطع وباسلوب القطع المتعامد، حيث أمكن وبالتفصيل محاكاة مايحدث في عملية القطع. ان عملية النمذجة والمحاكاة لعملية القطع تمت على أساس موديل رياضي اساسه نظرية الباحث (*Johnson*-

* Dept. of Production Eng. & Metallurgy, UOT.

https://doi.org/10.30684/etj.24.8A.13
2412-0758/University of Technology-Iraq, Baghdad, Iraq

Cook) والتي تعتبر ان سلوك المعدن خلال عملية القطع هو دالة للتصليد الانفعالي، معدل الانفعال ودرجة الحرارة وهو افتراض اقرب مايكون لما يحدث فعليا في عملية القطع من تأثيرات ديناميكية. أظهرت النتائج التحليلية في هذا البحث أن الضغط العمودي في منطقة تماس العدة مع النحاتة يكون أقل ما يمكن عندما تكون قيمة زاوية الجرف(5°)، في حين تكون قيمة الضغط أعلى مايمكن عند زاوية جرف مقدارها(15°-) ، حيث أمكن توضيح توزيع الضغط في هذه المنطقة بشكل تفصيلي. تم مقارنة هذه النتائج مع بحوث منشوره معتمدة وأظهرت وجود توافق كبير مع النتائج المستحصلة.

Nomenclature

- A The Static yield stress.
- A' The apparent area of contact.
- A_r The real area of contact
- B Hardening parameter.
- C Strain rate parameter.
- m Temperature exponent.
- n Strain Hardening exponent.
- μ A rate dependent Coulomb friction.
- μ_s Static coeff. of friction.
- μ_k Kinetic coeff. of friction.
- β' Exponent decay coeff..
- v Relative sliding velocity of the slave and master surfaces.
- σ The flow stress.
- $\dot{\bar{\varepsilon}}^*$ The non dimensional effective strain rate.
- $\bar{\varepsilon}$ The effective plastic strain.
- $\dot{\bar{\varepsilon}}$ The effective strain rate.
- $\dot{\varepsilon}_o$ The reference strain rate.
- T* The non dimensioned temp.
- T The working temp
- T_o The room temperature.

1. Introduction

In order to get further increase in the productivity and reduce costs, it is necessary to improve understanding of the machining process, since the machining system involves complexity of the physical phenomena, which occur over a wide range of temperatures, strains and strain rates. Modeling and simulation can increase the understanding of machining process. The simulation can reduce developing time and optimize costs, without the need for further machining tests. When metal is cut, the cutting force acts mainly through a small area of the rake face, which is in the contact with the chip and thus is known as the tool-chip interface. Therefore it is of interest in the cutting force determination and considerations of tool wear to determine the contact conditions at the tool-chip interface. To comprehend the contact process at this region, the following should be analyzed: the contact pressure (normal and shear) distribution, the temperature distribution, and the parameters of relative motion. Many studies have been carried out to reveal the normal and shear stresses at the tool-chip interface. A wide variety of experimental techniques including photoelastic tools, split-tool dynamometers, transparent tool for the direct observation of the tool-chip interface, metallurgical examination of 'quick-stop' chip section, experimental slip-line field method and others have been adopted [1-4].

Okushima et al [1971][5] used the photoelastic method and found that the whole contact length of tool-chip interface is divided into two distinctive parts of approximately equal length: the plastic part which extends from the cutting edge to the middle of the contact length and the elastic part from the middle of the contact to the point of chip separation. Their results indicated that the normal pressure being zero at the point of chip separation, then increases exponentially towards the cutting edge. The Finite Element Method (FEM) started to be applied in the simulation of metal cutting in the 1970's to improve the error generated by the slip-line solution, since the material was assumed to be rigid-perfectly plastic and the solution could not really account for the variation of yield stress with strain, strain rate and temperature. Some of these models gave information about stresses and strain fields, shear zones, temperature and stress distribution at tool-chip interface. Some models studied the effect of friction and forces at this region [6- 9].

Childs,T. et al,[1989][10] shows the variation of normal pressure at the tool face nodes along the tool-chip interface at the end of chip formation analysis using FEM. At the tool tip area, the normal pressure has the maximum value, then the distribution exhibits a plateau of high stress near the tool beyond the feed distance, the normal pressure drops sharply, when turning mild steel, at the distance of about (0.35 mm), the chip loses contact with the tool face, therefore the normal pressure drops to zero. *Kalhori.V.*,[2001][11] studied in brief the effect of the contact pressure at the tool-chip interface, using FEM and noticed that, the pressure will become several times the yield stress of the workpiece material, and this means that the real contact area between the tool and chip is so nearly complete over a large part of the total area of the interface, that sliding, as he stated at the interface is impossible, therefore the frictional force becomes that required to shear the weaker of the two material across the whole interface. This force is almost independent of normal force, but is directly proportional to apparent area of contact (A_r); a relationship is opposed to that of classical friction concepts.

Al-Hashimi,[2002][12] studied chip formation using FEM codes with certain constant force for chip separation criteria, he studied the effect of rake angle on many field parameters, such as, effective plastic strain, cutting forces, tool-chip contact length, chip contraction coefficient and shear angle. His results show that the contact length increases as the rake angle is decreased. The maximum relative difference between simulated and measured values of contact length was less than (10%). *V.P. Astakhov et al*, [2004] [13] stated that, the uniform distribution of normal and shear stresses is the case in metal cutting. The tool-chip interface was modeled as a contact problem of indentation of the deformable work material by a rigid punch. They had proven that the distribution of normal and shear stresses is not uniform.

Lijing Xie, [2004][14], showed that the normal pressure at the position of tool face node can be obtained directly using FEM, he showed a new chip formation modeling method to simulate the entire process from the initial chip formation, chip growth to steady state using the code ABAQUS/ Explicit. His work was condensed on the tool wear estimation at turning and milling processes. A critical analysis of the above mentioned papers and other studies related to pressure distribution beyond those analyzed above shows that it is quite possible that actual pressures and pressure distribution may have not yet come to light due to significant scatter in the results obtained. Although there have been numerous studies on the orthogonal cutting model, most are limited to certain topics, such as the distribution of residual stress and temperature on the machined workpiece and cutting tool. Little research effort has been made to exploring the effect of the rake angle of the tool on the cutting process; in this paper the FEM is used to simulate the effect of rake angle on the machining process from the incipient cut of the tool into the workpiece until the formation of steady state cutting.

2. Finite Element Method Technique

Two special FEM codes (MSC FEA/Patran/V2004&MSCFEA/Dytran/V 2004) are used to model the metal cutting process. The codes are applied with certain modifications to suit with metal cutting principles. The first code is used for preprocessing & postprocessing, while the second one is used for the analysis stage. This selection is based on the following reasons: the explicit dynamic method was originally developed to analyze high-speed dynamic events that are extremely costly to analyze using implicit programs, such as ABAQUS/standard. The explicit dynamic method also has advantages over the implicit method in modeling complex contact problems and material with degradation and failure, which is essential to model a metal cutting process. The orthogonal metal cutting process was modeled in three parts:

2.1 Orthogonal Cutting Model

Solid modeling is done for the proposed model sets to be as in orthogonal cutting, including in general the mesh selection to a number of elements and nodes. The boundary conditions are applied to imitate real metal cutting process. Two types of Lagrangian elements are applied as follows:

1. 8-nodes (CHEXA), for solid elements to simulate the deformed material (workpiece) having six degrees of freedom per node translational and rotational in x, y and z directions. This element comes with hourglass control that is important in dealing with large deformation during metal cutting.
2. 4- nodes (CQUAD4), for shell elements with three degree of freedom per node: translation in the nodal x, y and z directions, to simulate the shell between the chip and workpiece, which is used for tying concept between chip and the workpiece under predetermined constant force criteria.

The cutting conditions were chosen as follows: [Depth of cut = 0.5 mm, width of cut = 0.5 mm, cutting speed = 200 m/min.]

The bottom element of the workpiece is restrained from moving in all directions. The cutting tool is modeled as perfectly rigid body, because most tool materials have significantly high elastic modulus, compared with large plastic deformation of workpiece, the elastic deflection of the cutting tool can be ignored. The boundary conditions are such that the tool can move freely in x-direction which in other degree of freedom is restricted .The metal machined in simulation is (AISI 1045 St.), whose physical and other thermal properties and constants needed for the specified FEM program are available in the mentioned codes. The cutting tools are assumed to be rigid with various rake angles :(-15°,-10°, -5°, 0°, 5°, 10°, 15°). a constant clearance angle is chosen to be (7°), and the nose radius of the cutting edge is equal to (0.045) mm. Other assumptions for the model include that the chip formation is continuous, the workpiece is stress free prior to the cutting operation, and that cutting tool wear and residual stress from phase transformation are ignored.

2.2 Friction at the Tool-Chip Interface

However in metal cutting process, it is generally observed that the mean coefficient of friction on the tool face varies considerably with the change in cutting speed, rake angle and so on. This results from the extreme conditions of metal cutting area where the normal pressure at the tool-chip interface is very high. According to reference [17] the ratio of the real area of contact (A_r) to the apparent area of contact (A') approaches or reaches (1) under cutting conditions, which is different from the application conditions of Coloumb's assumption. The contact surfaces in our models were assumed to be sliding and sticking. A friction force is also applied to each of the surfaces, parallel to the surface. The magnitude of the force during sliding is equal to the magnitude of the normal force multiplied by the coefficient of friction. A new model of friction is applied called a rate dependent Coulomb friction (μ) is expressed by the following relation:

$$\mu = \mu_k + (\mu_s - \mu_k)\, e^{-\beta' v}$$

where:(μ_s) is the static coefficient of friction;

(μ_k) is the kinetic coefficient of friction.

(β') is the exponent decay coefficient,

(v) is the relative sliding velocity of the slave and master surfaces. Due to several numerical tests, The optimum coefficients of friction in sticking and sliding regions are found to be (0.4 & 0.5) respectively and are estimated using *Zorev*'s stress distribution model [1], which is till now, the most extensive experimental model for friction estimation in metal cutting field.

2.3 Material Model

The workpiece material is assumed to be (AISI 1045 St). Due to the large plastic deformation to which the workpiece material is subjected in metal cutting process, workpiece material strain hardens. The isotropic hardening model is employed to model this behavior by defining flow stress (σ) as a function of plastic strain, strain rate and temperature. The following *Johnson-Cook* constitutive model was able to include the effective plastic strain, strain rate and the strain hardening effects under high machining temperature:

$$\sigma = (A + B\bar{\varepsilon}^{\,n})(1 + C \ln \dot{\bar{\varepsilon}}^{*})(1 - T^{*\,m})$$

where: $\dot{\bar{\varepsilon}}^{*}$ is the non dimensional effective strain rate = $\dot{\bar{\varepsilon}} / \dot{\varepsilon}_o$,

T* is the non dimensioned temperature = $(T - T_o) / (T_{melt} - T_o)$.

$\bar{\varepsilon}$ is the effective plastic strain, $\dot{\bar{\varepsilon}}$ is the effective strain rate, $\dot{\varepsilon}_o$ is the reference strain rate, **T** is the working temperature, T_o is the room temperature, T_{melt} is the melting temperature. *A*, *B*, C, *n*, and m are material parameters. These terms are determined from experimental results data over a wide range of strain rate data was taken from tests and *Hopkinson* bar tests documented in the literature. These parameters can be obtained for various materials found in the Johnson-Cook paper and from experimental data [15, 16]. The heat generation in this study assumes adiabatic condition, as about 90% of the plastic work is converted to heat and about 60-70% of the heat generated goes into chip [18].

3. Results and Discussion

In Our models, the modeling and simulation process is classified into two stages, the first is non steady state that includes [initial contact, intimate contact and start of separation], while the second stage which represents the actual chip formation process is called steady state stage. Fig.(1) shows an example of the entire pressure distribution for the whole simulation time representing the two mentioned stages of chip formation process. The pressure fluctuation is shown dynamically then approaches a constant value as the tool advances through the workpiece to reach the steady conditions. The analytical results of the present modeling process show that the distribution of the normal pressure follow that obtained experimentally by Zorev[1].

Fig.(2)(A&B) shows the simulated chip contour and mesh deformation under different values of the following rake angles (-15°, -10°, -5°, 0°, 5°,10°, and 15°). We can see that as the rake angle is increased the normal pressure is decreased. As the tool rake angle increases from (-15° to +15°), the difference between chip thicknesses and undeformed chip thickness decreases, i.e. the larger the rake angle, the smaller the difference between the machined chip thickness and the original undeformed chip thickness. The pressure distribution in Fig.(2)(A&B) is shown by removing the tool from the model, as the rake angle is increased in the range of (-15° to 0°), a sharp pressure drop occurs from (1716 - 998) MPa, the reason is due to sticking or seizure at this region near the tool tip ranging at a distance from the tool tip to the in the mid distance of contact, which ensures that, the pressure at this region is reduced linearly due to force decomposition and change in contact area, so we can say that: Larger contact area can be seen using the cutting tool with smaller rake angles, reaching to quasi constant values in the range of (5° to 15°), so that the value of normal pressure is within the range of (562-773) MPa, which means also that, less sticking conditions may appear at this region. Further, it can be seen from Fig.(2)(A&B), that the chip tip surface also becomes smoother as the rake angle increases and the chip flows away from the cutting edge on both sides, the mesh deformation at the starting end of the machined workpiece shifts toward the left instead of the right, as for the above phenomena is that given a small rake angle, the cutting action after transform into pushing and squeezing force. In this case, a larger cutting force is required. This is also why there is a less smooth surface on the chip tip. In general, we can say that the cutting process can be affected by controlling the contact length of tool-chip interface when the contact is controlled to a certain length, so that the real contact is shorter than the natural contact, the cutting force is reduced. Consequently the specific horsepower of the workpiece as well as the tool temperature is reduced.

Fig.(3) shows comparison between the tool rake angle and maximum pressure at tool-chip interface for steady stage of chip formation process, the values of pressure drops to (1/3) in the range of rake angles (-15° to 5°), compared with that of range of rake angle (5° to 15°), leading to less tool wear and better tool life.

From this curve we can conclude that, the optimum rake angle that gives minimum normal pressure at tool-chip interface is (5 °), this may be caused by uniform pressure distribution caused by uniform contact criteria and thermal effects at this region, which means that low tool wear and high tool life for this rake angle. The mentioned description of pressure distribution is similar to the experimental tests being published in references [19, 20]. Fig.(4) (a & b) shows in detail the experimental pressure distribution along the area of contact as if the cutting was in progress, many observations can be seen, the contact area between the rake face and the chip is divided into three zones, next to the cutting edge, the chip was found to slide over the rake face with no metal transfer to the tool although there was intimate contact between the rake face and the freshly generated chips. The following zone can be seen clearly extending until the end of contact, there was a large decrease in pressure values, which is confirmed also by Fig.(5)[19].Fig.(5) shows photographs taken by camera with four frames using transparent cutting tools enabled the tool-chip contact area on the rake surface to be observed in situ during cutting using a high powered microscope. Multiple experiments studies conducted by references [22, 23, and 24] and many others conclusively proved that the tool-chip interface consists of the parts, namely the plastic part of the tool-chip interface can be clearly observed on the tool rake face. Therefore the uniform pressure distribution can be easily and clearly observed from Fig.(6)[22].

Fig.(7) shows in detail distribution behavior of normal pressure along the tool rake face for different values of rake angles. It can be seen that the normal pressure for negative rake angles is much greater than that for positive rake angles due the reasons being mentioned, this behavior for various rake angles can be explained as follows:

For rake angles in the range of (-15 °, --10 °, - 5 °), the distribution follows nearly exponential curve with the maximum at the cutting edge and zero at the point of separation, this distribution is similar to that being mentioned in references[25,26,27], Fig.(8)-curve3, shows the behavior details, experimental techniques are used in analyzing the normal pressure at tool-chip interface, using photoelastic method and split tool dynamometer with conditions similar to that used in the present paper.

Our modeled results agree well with Reference [14], who used FEM in his work, the machining conditions were as follows: orthogonal cutting, turning operation, dry cutting, Rake angle = -7 °,Work material: (AISI 1045 St.), Cutting parameters: V_c =300m/min, a=2mm, s=0.145 mm/rev. Fig.(8) shows the graph of the modeled results obtained from reference[4].

For rake angles in the range of (0 °,5°, 10 °,15 °) the curve trend is shown to be more steady in the region between the tool edge to one third of the contact region measured from the tool tip, then the pressure is dropped to zero at the end of contact region. This also agree well with references [25, 26, 28, 29], Fig.(8)-curve1, shows the detail description.

4. Conclusions

The main conclusions which may be drawn from the present simulation work are as follows

The optimum rake angle that gives minimum pressure under steady state stage is (5°), while the maximum pressure is recorded when the rake angle is (-15 °C).

1. The results of FEM modeling in which the actual experimental results obtained in orthogonal cutting tests were utilized fully support the results of the analytical modeling.
2. Pressure distribution of the normal pressure for negative rake angles (-15 °, -10°, -5°) follows nearly exponential curve with the maximum at the cutting edge and zero at the point of separation
3. For positive rake angles and zero (0 °, 5 °, 10 °, 15 °), the normal pressure distribution is more steady in the tool edge to one third of the contact region measured from the tool tip.
4. Predictions show that the present FEM code used for orthogonal cutting is an accurate viable analysis, as long as flow stress behavior of the work material is obtained realistically and friction at the chip-tool interface is modeled correctly.

5. References

1. Zorev N.N., Mechanics. Edited by M.C. Shaw, Pergamon Press, Oxford, 1966.
2. Oxley P.L.B., Mechanics of machining: An Analytical Approach to Assessing Machinability, John Wiley & Sons, New York, USA, 1989.
3. Astakhov V.P., Metal cutting mechanics, CRS Press, Boca Raton, USA, 1998.
4. Arsecularatne J.A., On tool-chip interface stress distribution, ploughing force and size effect in machining, International Journal of Machine Tools and Manufacture, Vol.37, No.7, pp.885 - 899, 1997.
5. Okushima,k., Kakino,y., Hahiha,S., Hasimoto,h., A stress analysis in the orthogonal cutting by photo elasto-plasticity method, Bulletting of Japanese Society of Precision Engineering, Vol.5, pp.1-7, 1971.
6. Strenkowski J. S. and Carrol J.T. III, A Finite Element Model of Orthogonal Metal Cutting, Trans. Journal of Eng. Ind., Vol. 107 No.4, pp. 346-354, 1985.
7. Shih A. J. M., Chandrasekar S. and Yang,H. T. Y. Finite element simulation of metal cutting process with strain rate and temperature effects, Fundamental Issues in Machining, ASME Publication, Vol.43, pp.11-24, 1990.
8. Shih A. J., Finite Element Simulation of Orthogonal Cutting, Journal of Engineering for Industry, Vol.117, pp.84-93, 1995.
9. Mackerle J., Finite Element Analysis and Simulation of Machining: A Bibliography (1976-1996), Journal of Materials Processing Technology, Vol.86, pp.17-44, 1999.
10. Childs,T., Mahdi, M., On The Stress Distribution Between The Chip and The Tool During Metal Turning, Ann. CIRP, Vol.38(1), pp.55-58, 1989.
11. Kalhori, V., Modeling and Simulation of Mechanical Cutting, Ph.D Thesis, Lulea, University of Technology, Sweden, 2001.
12. Al-Hashimi, M. A. T., Finite Element Simulation of Chip Formation and Comparison With Machining Experiments, Ph.D. Thesis, Submitted to the Department of Production Eng. and Metallurgy, University of

Technology, Baghdad, Iraq, Oct, 2002.

13. Astakhov V.P., Outerio J.C., Modeling of Contact Stress Distribution at The Tool-Chip Interface, Proceedings of 7[th] International Workshop of Modeling and Machining Operations, ENSAM, Clunty, France, 3-4 May 2004.
14. Lijing Xie, Estimation of Two-Dimensional Tool Wear Based On Finite Element Method, Ph.D. Thesis, University of Karlsruhe (TH), wbk Institute for Production Technique, 2004 .
15. Tugrul ozel, Erol Zeren, Determination of Work Material Flow Stress and Friction For FEA of Machining Using Orthogonal Cutting Tests, Journal of Material Processing Technology, 2004.
16. Jaspers S.P.F.C., Dautzenberg J. H., Material Behavior In Conditions Similar To Metal Cutting In The Primary Shear Zone, J. Mater. Process. Technology, Vol.122, pp.322-330, 2002.
17. Finnie,I., Shaw, M.C., The Friction Process In Metal Cutting, Transaction of the ASME, Vol.78, pp.1649-1657,1956.
18. Yang Xiaoping, Liu C. Richard, Modeling titanium and its alloys, Machining Science and Technology, Vol.3,No.1, pp.107-139, 1999.
19. Ackroyd B., Chandra N. S., Krishnamurthy K., et al, Exploration of Contact Conditions In Machining, Proc. Instn. Mech. Engrs, Vol.215, Part B, pp.439-507, 2001.
20. Doyle E,Horn, J.G., Tabor, D., Frictional Interaction Between Chip and Rake Conditions In Continuous Chipformation, Proc. R. Soc. Land. A., Vol.366, pp173-187, 1979.
21. Doyle.E, Horn, J.G., Tabor,D., Direct Observation of The Chip-Tool Interface In Metal Cutting, Inst. SME, Proceedings of The 5[th] North America Conference, pp.237-241, 1977.
22. Loladze T.N., Strength and Wear of Cutting Tools, (in Russian), Mashgiz, Moscow, 1958.
23. Poletica M.F., Contact Loads on Tool Interfaces, (in Russian), Mashinostroenie,Moskow, 1969.
24. Rice, W.B, Salmon R, Syniuta W.D., Photoelasticdetermination of cutting tool stress, Transactions of the E. I. C., Vol.4, No.(1), pp.20–23, 1960.
25. Chandrasekaran H, Kapoor D.V., Photoelastic Analysis oif Tool–Chip Interface Stresses, ASME Journal of Engineering for Industry, Vol.87, pp.495–502, 1965.
26. Bagchi A, Wright P.K., Stress Analysis In Machining With The Use of Sapphire Tools, Proceedings of The Royal Society of London A, Vol.113, pp.409-499, 1987.
27. Buryta D, Sowerby R., Yellowley I.,Stress distributions on The Rake Face During Orthogonal Machin-ing, International Journal of Mechanical Tools Manufacturing, Vol.34, No.(4), pp.721–739, 1994.
28. Usui E., Takeyama H., A Photoelastic Analysis Of Machining Stresses, ASME Journal of Engineering for Industry, Vol.82, pp.303–308, 1960.
29. Kato S, Yamaguchi K, Yamada M., Stress Distribution at The Interface Between Tool and Chip In Machining, ASME Journal of Engineeringfor Industry,Vol.94, pp.683–689, 1972.

Table (1) Johnson-Cook parameters for (AISI 1045 St.)

Static yield stress (A)	**553.1 MPa**
Hardening parameter (B)	**600.8 MPa**
Strain rate parameter (c)	**0.0134 sec^{-1}**
Reference strain rate($\dot{\varepsilon}$)	**1.0 sec^{-1}**
Strain Hardening exponent (n)	**0.234**
Temperature exponent(m)	**1.0**
Melting temperature (T_{melt})	**1500 °C**
Room temperature (T_o)	**25 ° C**

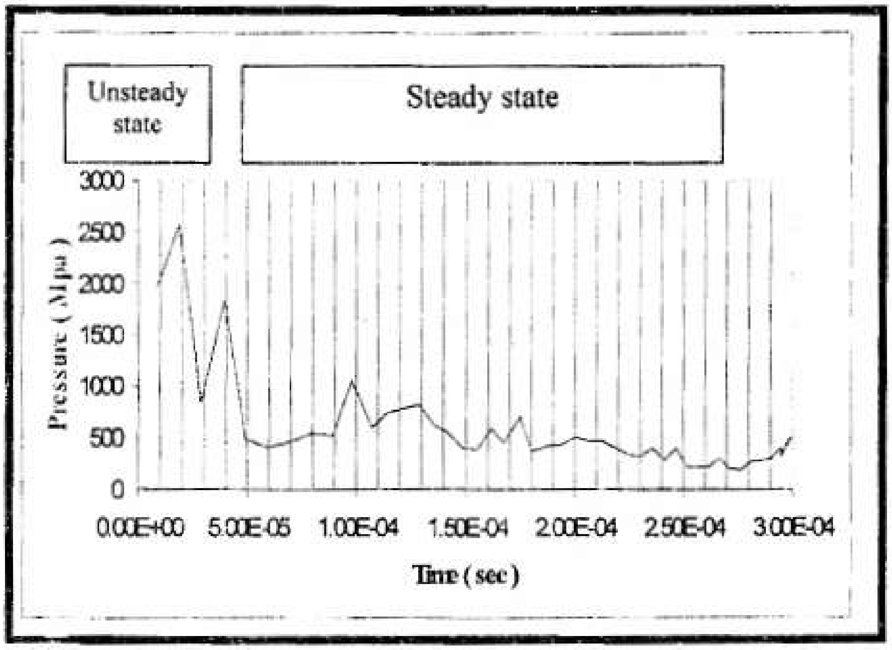

Fig.(1): Predicted pressure at tool-chip interface for total cutting time at different stages of chip formation process, (tool rake angle =15°).

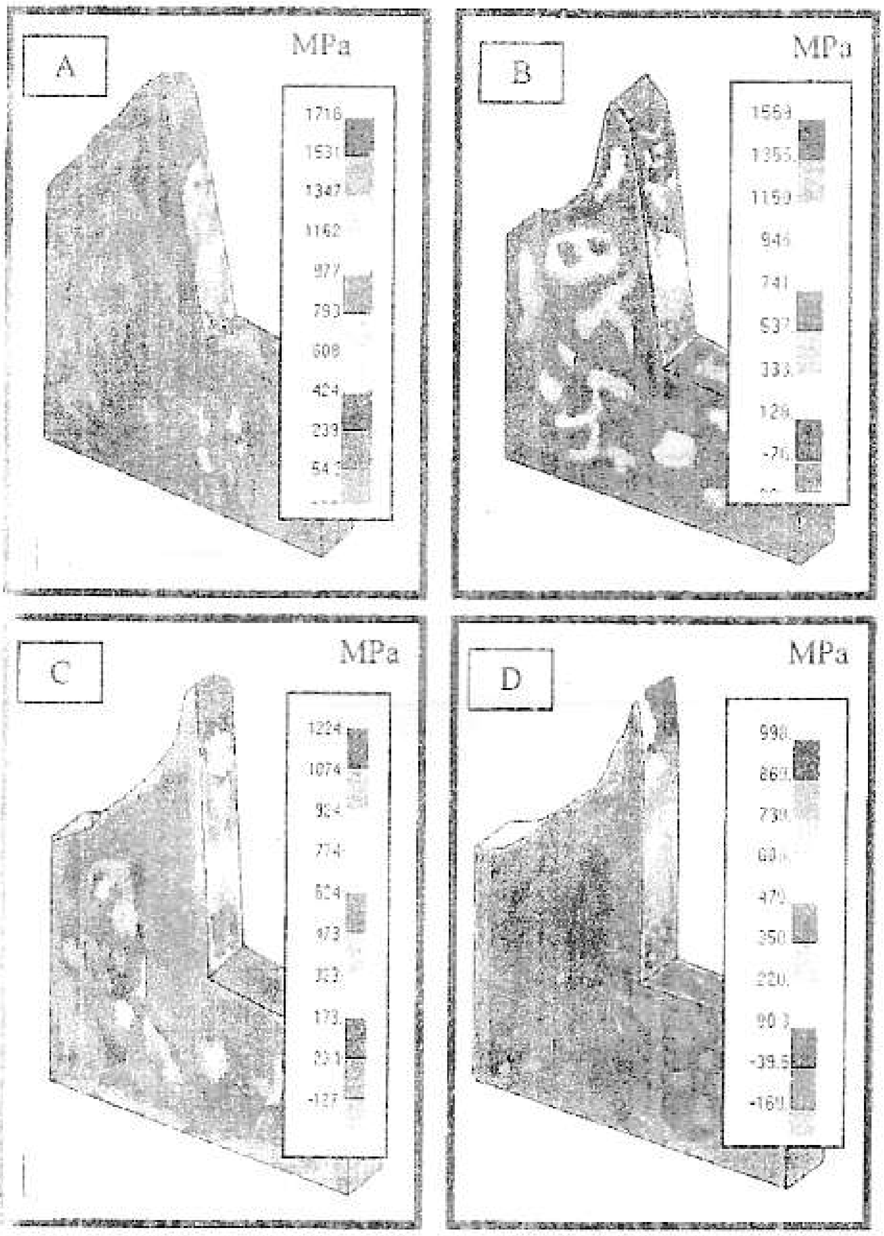

Fig.(2-A): FEA Pressure distribution(in MPa) at tool-chip interface for different rake angles at steady state stage of chip formation process (A = -15°, B = -10°, C = -5°, D = 0°).

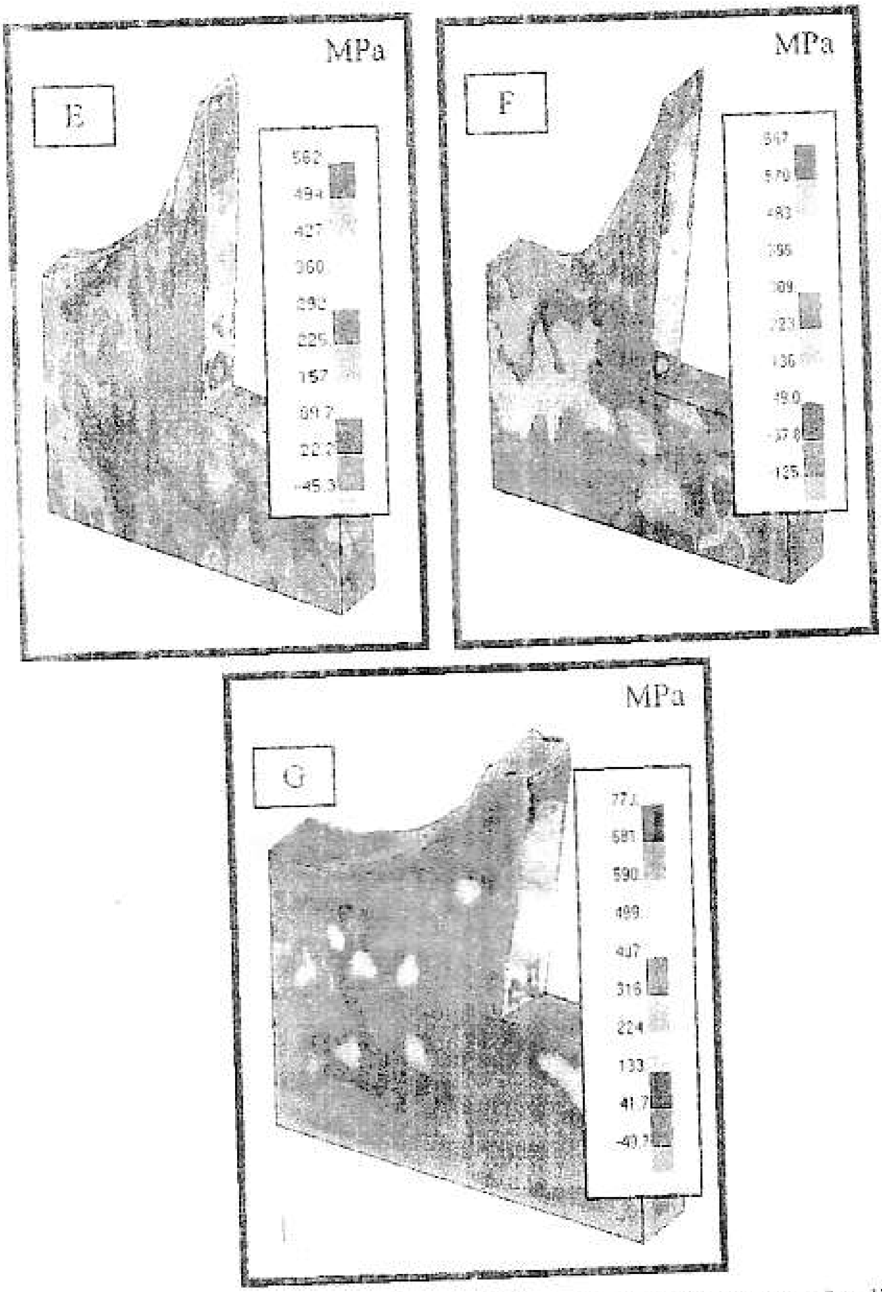

Fig.(2-B): FEA Pressure distribution(in MPa) at tool-chip interface for different rake angles at steady state stage of chip formation process. (E = 5°, F = 10°, G = 15°).

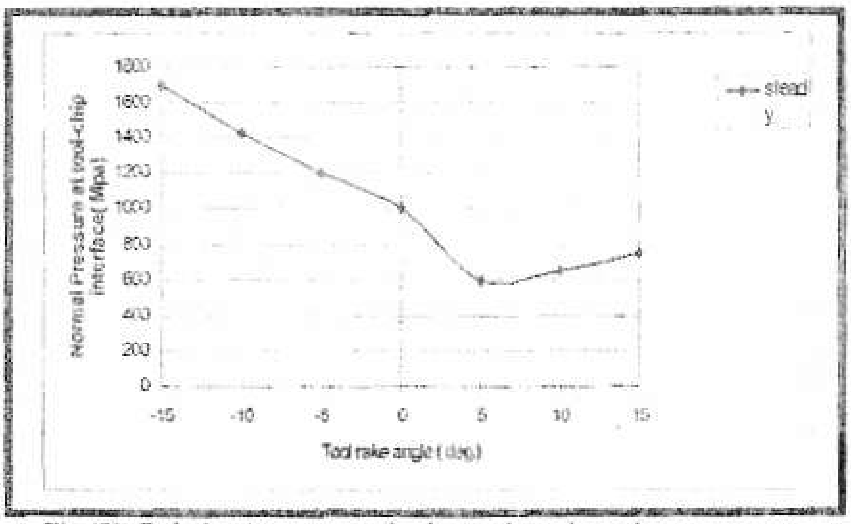

Fig.(3): Relation between tool rake angle and maximum pressure at tool-chip interface for steady stages of chip formation process.

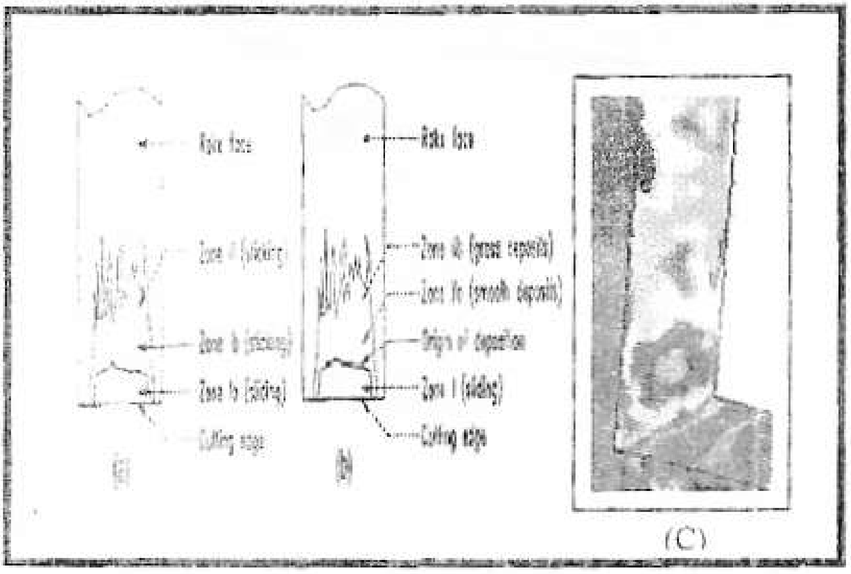

Fig.(4): Schematic diagram of the rake face showing extent of three distinct zones constituting the chip-tool contact area.

a- Classification adopted by reference [20]
b- Classification suggested by reference[19]
c- Current paper.

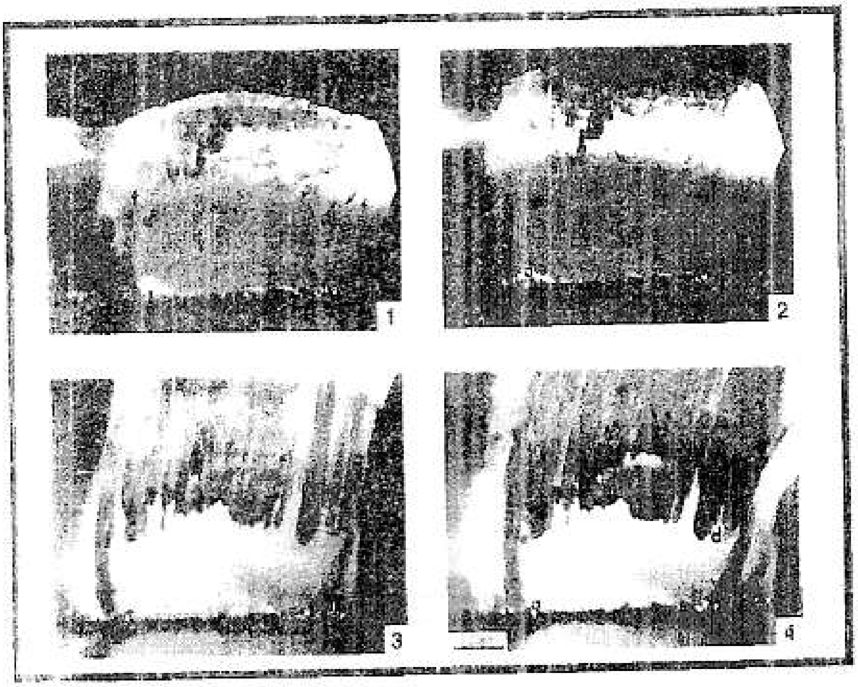

Fig.(5): Photographic sequence of the typical evolution of the chip-tool contact observed through a glass tool, showing the sliding and sticking zones [19].

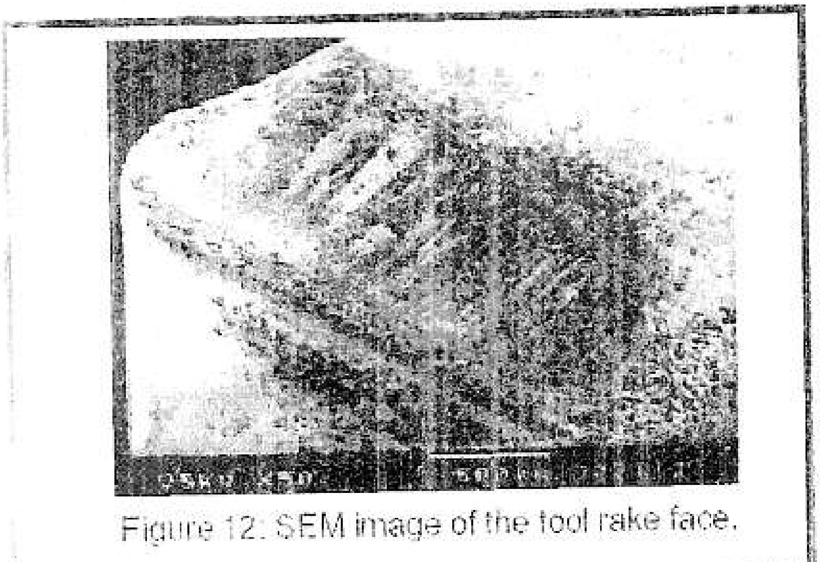

Fig.(6): SEM image of the tool rake face.[22].

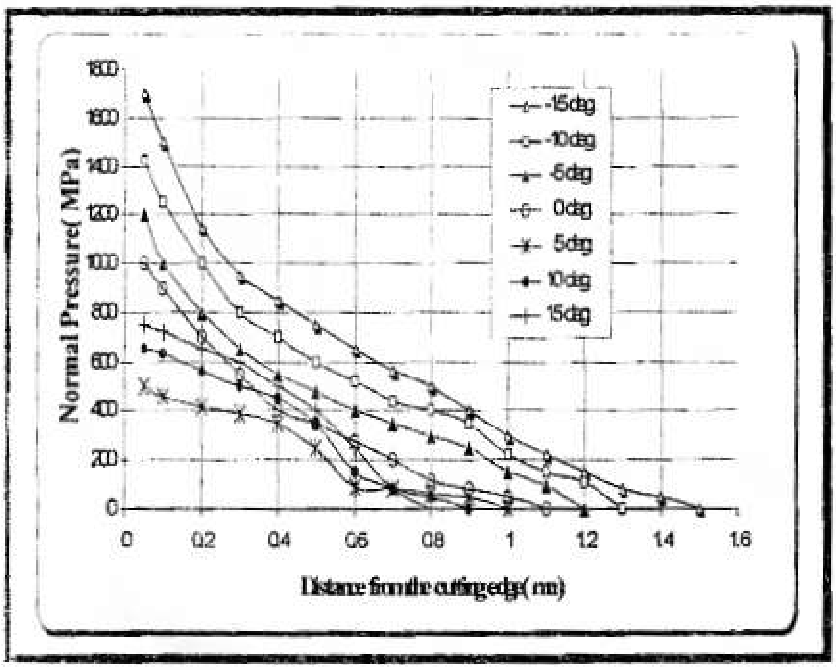

Fig.(7): Predicted normal pressure along the tool-chip interface for different values of rake angles.

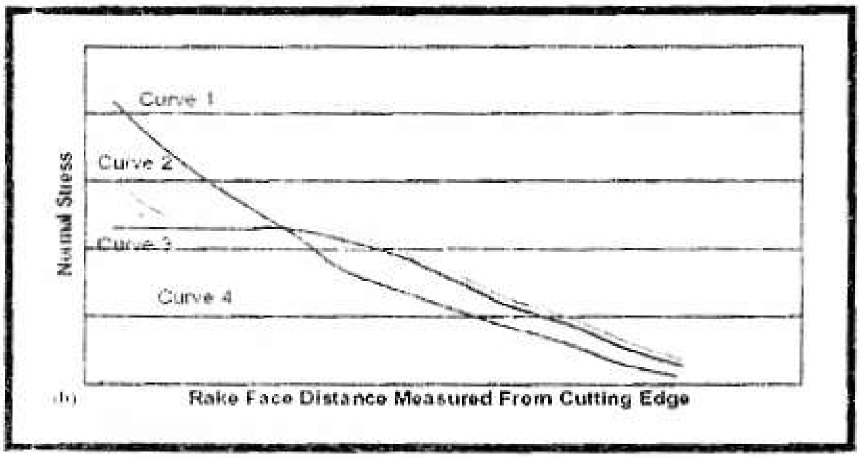

Fig.(8): Typical experimental pressure distribution at tool-chip interface[4].

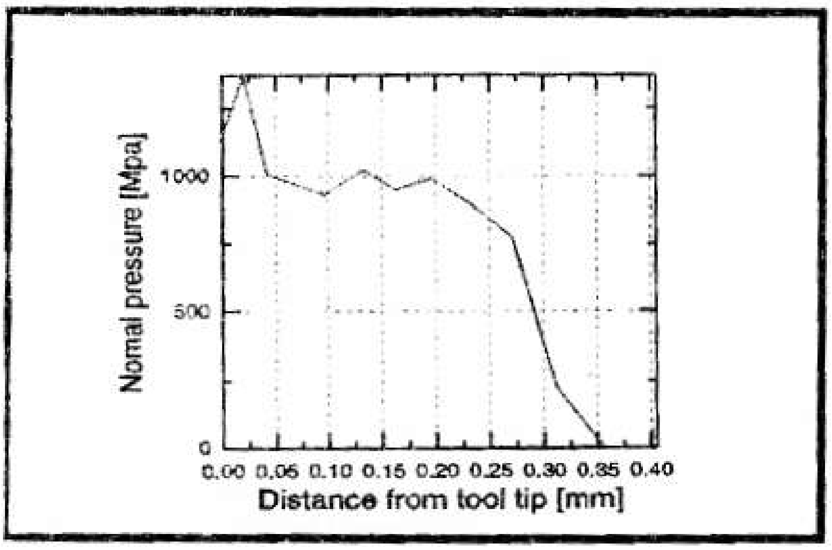

Fig.(9): Normal pressure of the tool face nodes at tool-chip interface at steady state [14].